Phase-resolved x-ray ferromagnetic resonance measurements of spin pumping in spin valve structures

M. K. Marcham,[1] L. R. Shelford,[2] S. A. Cavill,[2] P. S. Keatley,[1] W. Yu,[1] P. Shafer,[3] A. Neudert,[4] J. R. Childress,[5] J. A. Katine,[5] E. Arenholz,[3] N. D. Telling,[6] G. van der Laan,[2] and R. J. Hicken[1,*]

[1]*School of Physics and Astronomy, University of Exeter, Stocker Road, Exeter, Devon, EX4 4QL, United Kingdom*
[2]*Diamond Light Source, Harwell Science and Innovation Campus, Didcot, Oxfordshire, OX11 0DE, United Kingdom*
[3]*Advanced Light Source, Lawrence Berkeley National Laboratory, Berkeley, California 94720, USA*
[4]*Helmholtz-Zentrum Dresden-Rossendorf e. V., Institute of Ion Beam Physics and Materials Research, P.O. Box 51 01 09, 01314 Dresden, Germany*
[5]*San Jose Research Center, HGST, 3403 Yerba Buena Rd., San Jose, California 95135, USA*
[6]*Keele University, Institute for Science and Technology in Medicine, Guy Hilton Research Centre, Thornburrow Drive, Hartshill, Stoke-on-Trent, ST4 7QB, United Kingdom*

Element-specific phase-resolved x-ray ferromagnetic resonance (FMR) was used to study spin pumping within $Co_{50}Fe_{50}(3)/Cu(6)/Ni_{80}Fe_{20}(5)$ (thicknesses in nanometers) spin valve structures with large areas, so that edge effects typical of nanopillars used in standard magnetotransport experiments could be neglected. The phase of precession of the $Co_{50}Fe_{50}$ fixed layer was recorded as FMR was induced in the $Ni_{80}Fe_{20}$ free layer. The field dependence of the fixed layer phase contains a clear signature of spin transfer torque (STT) coupling due to spin pumping. Fitting the phase delay yields the spin-mixing conductance, the quantity that controls all spin transfer phenomena. The STT coupling is destroyed by insertion of Ta into the middle of the Cu layer.

The ability of a spin-polarized electric current to exert spin transfer torque (STT) upon a nanoscale ferromagnetic element has led to a revolution in electronics. Electrically addressed magnetic random access memory, agile microwave frequency spin transfer oscillators, and low power spintronic logic devices are being realized in metal-based structures, fueling research into spin-polarized transport in other classes of material. By also exploiting the spin Hall, spin Seebeck, and precessional spin-pumping effects, there are further opportunities to observe new physical effects and construct devices based upon the flow of pure spin currents. While microscopic theory for the generation, transfer, and absorption of spin current has been developed, it now needs to be tested in materials of practical interest. However, the fabrication of nanostructured devices for spin-polarized current injection and lateral transport of spin current continues to be a formidable challenge. Although multilayered thin-film stacks can be deposited with atomic scale precision, additional patterning and ion milling processes are required to form nanopillars and lateral spin valves. Processing may modify the structural and magnetic properties, particularly at edges, in a manner that is difficult to characterize and control. Hence there is an urgent need to study spin transfer effects in large-area films of the highest structural quality, in which the effects of nanoscale patterning are absent or negligible. In this way the intrinsic interfacial and interlayer STT effects can be better characterized.

In the spin-pumping effect, magnetization precession within a ferromagnetic (FM) "source" layer pumps pure spin current into an adjacent nonmagnetic (NM) layer.[1] A nonlocal damping may result from spin scattering in the NM layer. However, if a second FM "sink" layer is added to form a spin valve structure, then the transverse component of the spin current may be absorbed by the sink, generating a STT that acts upon the sink, and further modifying the damping of the source. The STTs generated, by injection of either a spin-polarized charge current or a pure spin current, depend upon the spin-mixing conductance $g^{\uparrow\downarrow}$. Studies of spin pumping in large-area multilayered films can therefore be used to predict the performance of nanostructured STT devices.

Spin pumping was first observed as an increased damping of the source layer in ferromagnetic resonance (FMR) experiments.[2] By varying the thickness of the sink layer, the transverse spin relaxation length within the sink layer has recently been inferred.[3] However, spin current can be destroyed by spin-flip scattering at interfaces and within the spacer layer. Therefore it is essential to also directly observe the response of the sink if the flow of spin current is to be fully understood. The dynamics of the sink have been detected in just a few time-resolved magneto-optical Kerr effect (TRMOKE) studies[4–6] of epitaxial structures with Ag and Au spacer layers. In this Rapid Communication we present x-ray ferromagnetic resonance (XFMR) measurements of spin pumping within spin valve structures with polycrystalline Cu spacer layers. Element-specific x-ray magnetic circular dichroism (XMCD) allows the magnetization dynamics of the source and sink layers to be studied independently. It will be shown that the field-dependent phase of precession of the sink layer provides a clear signature of STT coupling from which the value of $g^{\uparrow\downarrow}$ may be determined. The present study hence shows how phase-resolved measurements made upon each oscillator within an ensemble can provide information about their mutual interactions. This method has immediate extensions within acoustics,[7] plasmonics,[8] and the interaction of spins in quantum dots coupled by tunneling.[9]

A spin valve stack consisting of underlayers/ $Ta(3)/Ru(2)/Ir_{80}Mn_{20}(6)/Co_{50}Fe_{50}(3)/Cu(6)/Ni_{80}Fe_{20}(5)/Ru(7)$ (thicknesses in nm) was deposited by magnetron
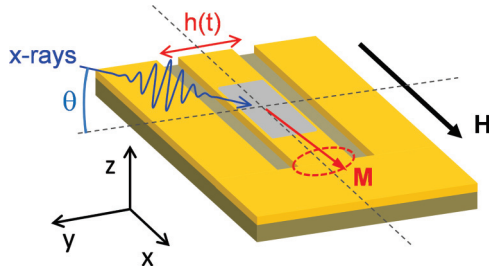
FIG. 1. (Color online) Schematic of the experimental geometry for XFMR measurements. Precession of the magnetization **M** about the bias field **H** is induced by an in-plane rf magnetic field **h**(*t*). The x-ray beam is incident at grazing angle θ.

FIG. 2. (Color online) Longitudinal MOKE loops acquired from the patterned structures with (a) the Cu spacer and (b) the Cu/Ta/Cu spacer.

sputtering onto an insulating sapphire substrate of 500 μm thickness. Field annealing was used to set the exchange bias field of the antiferromagnetic IrMn layer. The thickness of the Cu spacer layer is small compared to the spin diffusion length (350 nm).[10] However, a second reference stack was deposited with a Cu(2.5)/Ta(1)/Cu(2.5) spacer layer, in which strong spin scattering at the Ta is expected to quench the spin accumulation within the NM layer and suppress STT-induced dynamics of the sink. A combination of electron-beam lithography and ion-beam milling was used to pattern the magnetic layers of the stack into elements with lateral dimensions of 190 $\times$ 400 μm^2. Photolithography and further milling were then used to define a 50 Ω coplanar waveguide (CPW) within the now exposed nonmagnetic Ta(5)/[Cu(25)/Ta(3)]$_{\times 3}$/Cu(25)/Ta(5)/Ru(10) underlayers. The elements are sufficiently large that inhomogeneities associated with edges make negligible contribution to the spatially averaged behavior of the element. A 5-μm border was left between the edges of the element and the central track of the CPW to avoid any significant out-of-plane field excitation.

Phase-resolved XFMR measurements were made in fluorescence yield.[11] A continuous wave microwave magnetic field was phase locked to the x-ray pulse train generated by the synchrotron and used to excite the sample magnetization into a state of steady precession about an in-plane bias magnetic field. The sample was positioned close to the shorted end of the CPW, as shown in Fig. 1, so as to be close to an antinode of the microwave field. The exchange bias field and the applied field lay parallel to the length of the CPW in the experiment, of which further details are given elsewhere.[11]

Previous TRMOKE studies of the STT-induced dynamics of the sink layer used a spacer of sufficient thickness that the MOKE signal from the source layer was negligible.[5] Other studies used a rotatable compensator to suppress the signal from the source layer.[4,6] In this XFMR study the response of the source and sink layers is distinguished by tuning the x-ray energy to the Ni L_3 edge and Co L_3 edge, respectively.

Theory[12] predicts that the FMR linewidth of the source will be broadened as it "leaks" spin angular momentum into the adjacent NM layer. The pure spin current pumped into the NM layer generates a spin accumulation that may be described as a spin splitting of the chemical potential when diffuse scattering at the interfaces randomizes the electron momentum within the NM layer.[13] Spin currents driven by diffusion within the
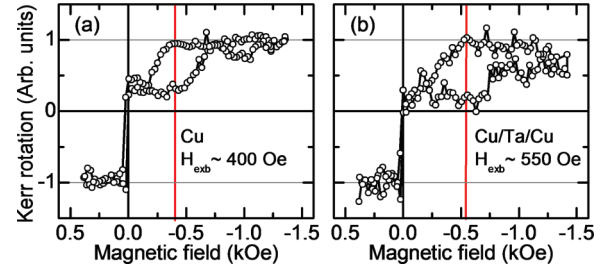
NM layer flow both in to the sink and back to the source. The back flow partially (fully) compensates the spin current from the source when its magnetization is precessing (in equilibrium). It is assumed that spin current injected into a 3*d* transition-metal FM layer is completely absorbed near the interface. The absorption of the component of spin angular momentum transverse to the sink magnetization generates a STT. The equations of motion take the form of coupled Landau-Lifshitz-Gilbert equations modified to include STT due to spin pumping,[2]

$$\frac{\partial \mathbf{m}_i}{\partial t} = -|\gamma_i|\mathbf{m}_i \times \mathbf{H}_{\text{eff},i} + \alpha_i^{(0)}\mathbf{m}_i \times \frac{\partial \mathbf{m}_i}{\partial t}$$
$$+ \alpha_i^{\text{SP}}\left[\mathbf{m}_i \times \frac{\partial \mathbf{m}_i}{\partial t} - \mathbf{m}_j \times \frac{\partial \mathbf{m}_j}{\partial t}\right], \quad (1)$$

where $\mathbf{m}_i$ and $\mathbf{m}_j$ are unit vectors parallel to the magnetization vectors of layers *i* and *j*, respectively. The first term on the right-hand side represents the torque term due to the local effective field $\mathbf{H}_{\text{eff},i}$, while the second represents the damping within the *i*th layer due to intrinsic spin-orbit effects and two magnon scattering. The third term describes the enhanced damping of the *i*th layer due to spin pumping, while the fourth term represents the STT induced by absorption of spin current from the *j*th layer.

Let us consider the case that the resonance field of the fixed layer ($i = 2$) lies below that of the free layer ($j = 1$), and is heavily damped so that the fixed and free layer resonances overlap. The direction of the STT acting upon the fixed layer changes abruptly as the field passes through the free layer resonance value. Above (below) the free layer resonance the difference in phase between the precession of the fixed layer and the oscillation of the driving field decreases (increases) as the STT partially assists (opposes) the torque term due to the static applied field. The magnitude of the STT scales with the amplitude of the free layer precession, and so, to a first approximation, the STT generates a bipolar feature in the field-dependent fixed layer phase that has a width comparable to the FWHM of the free layer resonance. Outside this field range the fixed layer phase returns to the background value resulting from excitation of the fixed layer by the rf field.

The longitudinal MOKE hysteresis loops acquired from the patterned samples are shown in Fig. 2. All dynamic measurements were performed for positive bias field, where the free and fixed layer magnetizations are parallel. The free layer resonance condition was identified by sweeping the bias field with the delay between the x rays and microwaves set
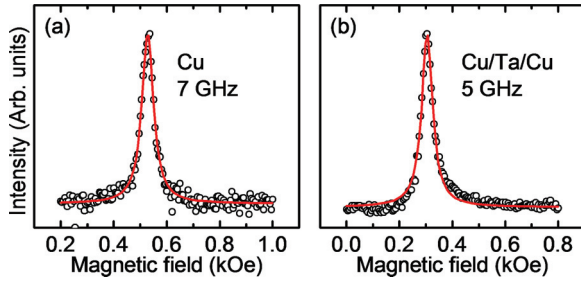
FIG. 3. (Color online) (a) The imaginary component of the magnetic susceptibility component χ_{yy} of the free layer for (a) the Cu spacer at 7 GHz and (b) the Cu/Ta/Cu spacer at 5 GHz. Lorentzian fits to the experimental data (open symbols) are shown as solid red curves.

so as to obtain the imaginary component of the magnetic susceptibility component χ_{yy} as shown in Fig. 3.

The linewidth extracted by Lorentzian fitting was found to be equal to 50 Oe for both samples within experimental error. At 7 GHz [Fig. 3(a)] this requires the sum of the damping constants $\alpha_1^{(0)}$ and α_1^{SP} for the free layer to be equal to 0.0105. Due to imperfect impedance matching the microwave amplitude at the sample had a different frequency dependence for each sample. Excitation frequencies of 7 and 5 GHz were used in Figs. 3(a) and 3(b), respectively, for which the microwave amplitude was a maximum in each case. In Fig. 3(b) a linewidth of 50 Oe at 5 GHz implies that the sum of the damping parameters is equal to 0.0150. Although no attempt is made to separate the contributions to the damping, the damping of the free layer in the absence of spin pumping is expected to be similar at 5 and 7 GHz. This suggests that the value of α_1^{SP} is larger for the Cu/Ta/Cu spacer, as expected if the Ta strongly scatters spins within the spacer layer. The spin-pumping contribution to the Gilbert damping coefficient has the form[14]

$$\alpha_i^{\mathrm{SP}} = \frac{g\mu_B \mathrm{Re}(g^{\uparrow\downarrow})}{8\pi M_i d_i}, \tag{2}$$

where M_i is the saturation magnetization, d_i is the layer thickness, g is the spectroscopic splitting factor, and $\mathrm{Re}(g^{\uparrow\downarrow})$ is the real part of the spin-mixing conductance, which has not been corrected to account for the Sharvin conductance.[12]

The fixed layer resonance was not observable in field sweep measurements performed on either sample due to a large damping resulting from direct contact with the IrMn. However, the precession of the fixed layer could be observed in time delay scans performed at different applied fields as shown in Fig. 4. The phase of the x-ray pulses relative to the microwave field was varied by passing the microwaves through an electromechanical delay generator. The delay scans obtained from the Cu and Cu/Ta/Cu samples are shown in Figs. 4(a) and 4(b), respectively. A sine curve with period equal to that of the microwaves was fitted to each scan. A background of constant phase and amplitude, arising from inductive pickup, was subtracted from the fitted curves. The fitted amplitudes are plotted against the applied field in Figs. 4(c) and 4(d). The phase of each fitted curve relative to the microwave field is plotted in Figs. 4(e) and 4(f). Free layer delay scans (not shown) were also fitted and the phase
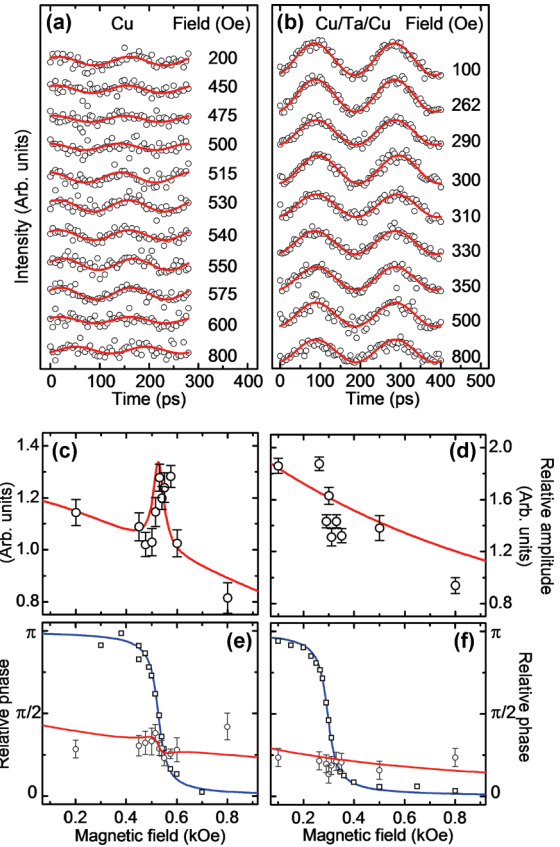

FIG. 4. (Color online) Fixed (sink) layer delay scans for (a) the Cu spacer at 7 GHz and (b) the Cu/Ta/Cu spacer at 5 GHz. The sine curves (red) are fits to the data (open dots). (c), (d) Fitted amplitudes are plotted as open dots. (e), (f) The phase relative to the driving field of both fixed (open circles) and free (open squares) layers is plotted. The red (fixed layer) and blue (free layer) curves assume (e) $\alpha_1^{\mathrm{SP}} = 0.0050$ and $\alpha_2^{\mathrm{SP}} = 0.0034$; (f) $\alpha_1^{\mathrm{SP}} = 0.010$ and $\alpha_2^{\mathrm{SP}} = 0.0068$.

values are plotted for comparison. No background subtraction was performed for the much larger free layer signals. The free layer phase curve has the sigmoidal shape expected for a simple harmonic oscillator.

For the Cu spacer, a clear peak at the free layer resonance (530 Oe) is observed in Fig. 4(c) on top of a broad Lorentzian background due to the FMR of the fixed layer. No clear peak is seen for the control sample [Fig. 4(d)]. For the Cu spacer, a clear bipolar variation in the phase due to STT coupling is observed at the free layer resonance field. For the control sample there is perhaps a small dip in the fixed layer phase at the free layer resonance. A unipolar phase variation is characteristic of dipolar coupling, resulting from interfacial roughness, or interlayer exchange coupling, although the latter is expected to be negligible for a 6 nm Cu thickness.

The amplitude and phase data in Fig. 4 were modeled with a linearized macrospin solution of Eq. (1). The saturation magnetization of the free and fixed layers was assumed to be 815 and 2017 emu cm^{-3}, as determined by vibrating sample magnetometry measurements made on coupon samples, while the exchange bias field was taken from the loops in Fig. 2. Dipolar coupling between fixed and free layers was neglected. The

fixed layer damping constant $\alpha_2^{(0)}$ was varied so as to reproduce the background for the fixed layer response, yielding values of 0.45 and 0.35 for Cu and Cu/Ta/Cu, respectively. These values are large but reasonable. A previous study[15] showed that the damping constant of a $Ni_{81}Fe_{19}/Fe_{50}Mn_{50}$ sample increased from 0.008 to 0.05 as the exchange bias field increased from 0 to 120 Oe. Extrapolating to the exchange bias values of Fig. 2 yields values for the damping constant comparable to those obtained here.

The linewidths observed in Fig. 3 constrain the total free layer damping constant ($\alpha_1^{(0)} + \alpha_1^{SP}$) to values of 0.0105 and 0.0150 for the Cu and Cu/Ta/Cu samples, respectively. The values of α_1^{SP} and $\alpha_1^{(0)}$ were varied subject to this constraint to give the best simultaneous agreement with the free and fixed layer responses in Fig. 4. The best agreement for the Cu sample was obtained when $\alpha_1^{(0)} = 0.0055$ and $\alpha_1^{SP} = 0.0050$. From Eq. (2) this implies that $\alpha_2^{SP} = 0.0034$. The intrinsic Gilbert damping of $\alpha_1^{(0)} = 0.0055$ for permalloy is in agreement with the range of values reported in the literature.[16] We note that the values for α_1^{SP} and α_2^{SP} are also comparable to those found in previous spin-pumping studies ($3 - 5 \times 10^{-3}$).[4] The curves in Fig. 4(f) were obtained with $\alpha_1^{(0)} = 0.005$ and $\alpha_1^{SP} = 0.010$. This then implies that $\alpha_2^{SP} = 0.0068$. However, since no evidence of STT was observed in the Cu/Ta/Cu sample, the fourth term on the right-hand side of Eq. (1) was set to zero for both layers. The implication is that strong spin scattering in the Ta layer prevents spin current passing from one layer to the other.

Inserting the fitted α_1^{SP} into Eq. (2) yields $\mathrm{Re}(g^{\uparrow\downarrow}) = 2.64 \times 10^{15}$ cm^{-2}. The value of $\mathrm{Re}(g^{\uparrow\downarrow})$ is related to the number of conducting channels per spin and is a measure of the spin-pumping efficiency.[17] Approximate expressions of $\mathrm{Re}(g^{\uparrow\downarrow}) \approx 1.2 n^{2/3}$ and $0.75 n^{2/3}$ have been assumed previously[14,18] where n is the number of electrons per spin in the spacer layer. Assuming $n = 4.25 \times 10^{22}$ cm^{-3} for Cu (Ref. 19) leads to $\mathrm{Re}(g^{\uparrow\downarrow}) = 1.46$ and 0.91×10^{15} cm^{-2}, respectively. Improved agreement can be expected following correction for the Sharvin conductance[14] but this requires input from *ab initio* electronic structure calculations that lie beyond the scope of the present study. Strictly speaking a separate value of $g^{\uparrow\downarrow}$ should be introduced to describe each interface at which spin scattering can be expected to occur. Therefore the values deduced here should be regarded as effective values that describe the two dissimilar interfaces and any internal structure of the spacer layer.

In summary, phase-resolved XFMR measurements of the spin-pumping effect have been demonstrated for spin valve structures with polycrystalline Cu spacers. The field-dependent phase of precession of the fixed layer at the free layer resonance provides a clear signature of STT coupling due to spin pumping. The phase variation is reproduced by a macrospin model that allows the real part of the spin-mixing conductance to be determined. By quantifying the flow of spin angular momentum from the source layer and into the sink layer, XFMR is a powerful new tool for the study of spin transfer in material systems of practical interest. The present work illustrates the more general principle of how measuring the phase of individual oscillators within an ensemble can provide unique insight into their mutual interaction.

*R.J.Hicken@exeter.ac.uk

[1] Y. Tserkovnyak, A. Brataas, and G. E. W. Bauer, Phys. Rev. Lett. **88**, 117601 (2002).

[2] B. Heinrich, Y. Tserkovnyak, G. Woltersdorf, A. Brataas, R. Urban, and G. E. W. Bauer, Phys. Rev. Lett. **90**, 187601 (2003).

[3] A. Ghosh, S. Auffret, U. Ebels, and W. E. Bailey, Phys. Rev. Lett. **109**, 127202 (2012).

[4] G. Woltersdorf, O. Mosendz, B. Heinrich, and C. H. Back, Phys. Rev. Lett. **99**, 246603 (2007).

[5] B. Kardasz, O. Mosendz, B. Heinrich, Z. Liu, and M. Freeman, J. Appl. Phys. **103**, 07C509 (2008).

[6] O. Mosendz, G. Woltersdorf, B. Kardasz, B. Heinrich, and C. H. Back, Phys. Rev. B **79**, 224412 (2009).

[7] J. F. Robillard, A. Devos, I. Roch-Jeune, and P. A. Mante, Phys. Rev. B **78**, 064302 (2008).

[8] E. Prodan, C. Radloff, N. J. Halas, and P. Nordlander, Science **302**, 419 (2003).

[9] D. Kim, S. G. Carter, A. Greilich, A. S. Bracker, and D. Gammon, Nat. Phys. **7**, 223 (2011).

[10] F. J. Jedema, A. T. Filip, and B. J. Van Wees, Nature (London) **410**, 345 (2001).

[11] M. K. Marcham, P. S. Keatley, A. Neudert, R. J. Hicken, S. A. Cavill, L. R. Shelford, G. van der Laan, N. D. Telling, J. R. Childress, J. A. Katine, P. Shafer, and E. Arenholz, J. Appl. Phys. **109**, 07D353 (2011).

[12] Y. Tserkovnyak, A. Brataas, G. E. W. Bauer, and B. I. Halperin, Rev. Mod. Phys. **77**, 1375 (2005).

[13] T. L. Monchesky, A. Enders, R. Urban, K. Myrtle, B. Heinrich, X.-G. Zhang, W. H. Butler, and J. Kirschner, Phys. Rev. B **71**, 214440 (2005).

[14] B. Kardasz and B. Heinrich, Phys. Rev. B **81**, 094409 (2010).

[15] M. C. Weber, H. Nembach, B. Hillebrands, and J. Fassbender, J. Appl. Phys. **97**, 10A701 (2005).

[16] S. S. Kalarickal, P. Krivosik, M. Wu, C. E. Patton, M. L. Schneider, P. Kabos, T. J. Silva, and J. P. Nibarger, J. Appl. Phys. **99**, 093909 (2006); K. Kobayashi, N. Inaba, N. Fujita, Y. Sudo, T. Tanaka, M. Ohtake, M. Futamoto, and F. Kirino, IEEE Trans. Magn. **45**, 9464 (2009); P. S. Keatley, V. V. Kruglyak, P. Gangmei, and R. J. Hicken, Phil. Trans. R. Soc. A **369**, 3115 (2011).

[17] T. Yoshino, K. Ando, K. Harii, H. Nakayama, Y. Kajiwara, and E. Saitoh, J. Phys.: Conf. Ser. **266**, 012115 (2011).

[18] B. Heinrich, C. Burrowes, E. Montoya, B. Kardasz, E. Girt, Y.-Y. Song, Y. Sun, and M. Wu, Phys. Rev. Lett. **107**, 066604 (2011).

[19] N. W. Ashcroft and N. D. Mermin, *Solid State Physics* (Holt, Rinehart and Winston, Philadelphia, 1976).